Received: 23 April 2022 | Revised: 10 August 2022 | Accepted: 21 August 2022

DOI: 10.1002/hbm.26063

RESEARCH ARTICLE

WILEY

Age-matched control or age-specific template, which is essential for voxel-wise analysis of cerebral metabolism abnormality in pediatric patients with epilepsy?

Yuankai Zhu[1] | Ge Ruan[2] | Sijuan Zou[1] | Luoxia Liu[1] | Xiaohua Zhu[1]

[1]Department of Nuclear Medicine and PET Center, Tongji Hospital, Tongji Medical College, Huazhong University of Science and Technology, Wuhan, China

[2]Department of Radiology, Hospital, Hubei University, Wuhan, China

Correspondence
Xiaohua Zhu, Department of Nuclear Medicine, Tongji Hospital, Tongji Medical College, Huazhong University of Science and Technology, No. 1095 Jiefang Ave, Wuhan 430030, China.
Email: evazhu@vip.sina.com

Funding information
National Natural Science Foundation of China, Grant/Award Numbers: 81801729, 81873903, 91959119

Abstract

The aim of this study was to explore the influences of age-matched control and/or age-specific template on voxel-wise analysis of brain ^{18}F-fluorodeoxyglucose positron emission tomography (^{18}F-FDG PET) data in pediatric epilepsy patients. We, retrospectively, included 538 pediatric (196 females; age range of 12 months to 18 years) and 35 adult subjects (18 females; age range of 20–50 years) without any cerebral pathology as pediatric and adult control group, respectively, as well as 109 pediatric patients with drug-resistant epilepsy (38 females; age range of 13 months to 18 years) as epilepsy group. Statistical parametric mapping (SPM) analysis for ^{18}F-FDG PET data of each epilepsy patients was performed in four types of procedures, by using age-matched controls with age-specific template, age-matched controls with adult template, adult controls with age-specific template or adult controls with adult template. The numbers of brain regions affected by artifacts among these four types of SPM analysis procedures were further compared. Any template being adopted, the artifacts were significantly less in SPM analysis procedures using age-matched controls than those using adult controls in each age range ($p < .001$ in each comparison), except in the age range of 15–18 ($p > .05$ in each comparison). No significant difference was found in artifacts, when compared procedures using the identical control group with different templates ($p = 1.000$ in each comparison). In conclusion, the age stratification for age-matched control should be divided as many layers as possible for the SPM analysis of brain ^{18}F-FDG PET images, especially in pediatric patients ≤14-year-old, while age-specific template is not mandatory.

KEYWORDS
epilepsy, pediatric, positron emission tomography (PET), statistical parametric mapping (SPM)

1 | INTRODUCTION

Epilepsy is a common chronic disease of central nervous system in children and adolescents (Beghi et al., 2019). Unfortunately, antiepileptic drugs are effective only in approximately 70% of these patients. Pediatric patients with drug-resistant epilepsy suffer from poor quality of life (Verrotti & Mazzocchetti, 2016). Neurosurgery, a widely accepted treatment option for drug-resistant epilepsy, can

render majority of selected patients seizure-free. Thus, timely access to tailored surgery for these patients is urgently needed (Lamberink et al., 2020).

Precise localization of the epileptic foci is one of the most critical procedure for epilepsy surgery. ^{18}F-fluorodeoxyglucose positron emission tomography (^{18}F-FDG PET) is a proven technique for the noninvasive localization of epileptic foci (Lagarde et al., 2020). Visual assessment is routinely applied in the qualitative analysis of brain ^{18}F-FDG PET images, whereas its accuracy highly depends on the expertise of nuclear medicine physicians. Statistical parametric mapping (SPM) approach, a computer-aided statistical software dedicated for neuroimage, enables higher reproducibility and reliability for the voxel-wise analysis of brain ^{18}F-FDG PET images (Bernasconi et al., 2016). This objective method has been widely utilized for interpreting brain ^{18}F-FDG PET data in adult patients with epilepsy, by using adult control and template (Chassoux et al., 2010; Kumar et al., 2021; Signorini et al., 1999). However, the age-related alterations of both brain contour and glucose metabolism pattern, may induce dramatic artifacts in the procedure of SPM analysis for pediatric patients, in the absence of age-matched control and corresponding template (Muzik et al., 2000). Several studies attempted to introduce pediatric patients with extracranial diseases as "pseudo-control" group, combined with pediatric brain template (Archambaud et al., 2013; De Blasi et al., 2018; Zhu et al., 2017). The respective influence of age-matched control or age-specific template on voxel-wise analysis of brain ^{18}F-FDG PET images in pediatric epilepsy patients has not yet been elucidated.

The aim of this retrospective study was to establish pediatric control database of brain ^{18}F-FDG PET images, accompanied by corresponding age-specific standard brain templates. In addition, the influences of age-matched control and/or age-specific template on interpreting brain ^{18}F-FDG PET data in pediatric epilepsy patients were explored.

2 | METHODS

2.1 | Participants

The pediatric control group was derived from patients without any cerebral pathology. The inclusion criteria were as follows: age ≤18; proven or suspected extracranial disease; whole-body ^{18}F-FDG PET/CT study with a separated brain scan (Archambaud et al., 2013; Zhu et al., 2017). A total of 1177 pediatric patients from December 2013 to June 2021 were, retrospectively, investigated. Patients were excluded, if they had any history of neuropsychiatric disorders, cerebral structural or glucose metabolism abnormality, or under treatment (chemotherapy or radiotherapy) (Hua et al., 2015). Finally, 538 pediatric patients (196 females; age range of 12 months to 18 years) were enrolled to build control data sets. Besides, 35 healthy subjects (18 females, ranging from 20 to 50 years) were introduced as adult control group.

A total of 112 pediatric patients with drug-resistant epilepsy referred to our institution for the evaluation of epileptic foci through dedicated brain ^{18}F-FDG PET/CT scans from December 2013 to June 2021, were, retrospectively, investigated. The inclusion criteria for epilepsy group consisted of confirmed diagnosis of drug-resistant epilepsy, age ≤18 years and comprehensive data of history (Kwan et al., 2010; Zhu et al., 2017). Since a wide range of brain tissue defect would hamper the normalization procedure in SPM analysis, 1 patient with porencephaly and 2 patients with head trauma were excluded. Among the 109 epileptic patients (38 females; age range of 13 months to 18 years) finally included, structural abnormalities were observed in 32 patients through MRI, including hippocampal sclerosis or atrophy ($n = 19$), cortical dysplasia ($n = 6$), arachnoid cyst ($n = 5$), and heterotopias ($n = 2$). The study design and exemption from informed consent were approved by the local Institutional Review Board.

2.2 | Image acquisition

All subjects were requested to fast for at least 4 h before PET/CT study, and the blood glucose levels were less than 160 mg/dl prior to ^{18}F-FDG administration (Varrone et al., 2009). Brain ^{18}F-FDG PET data were acquired in three-dimensional mode at 60 min after intravenous injection of ^{18}F-FDG (3.7 MBq/kg) using a PET/CT scanner (Discovery PET/CT Elite, GE Medical Systems) (Gelfand et al., 2011). For the control group, the routine whole-body ^{18}F-FDG PET/CT images were obtained with separated brain scan. The matrix size of reconstructed brain PET images was $192 \times 192 \times 47$ with a voxel size of $1.56 \times 1.56 \times 3.27$ mm^3, using a fully three-dimensional iterative reconstruction algorithm of SharpIR + VUE point HD with 2 iterations and 24 subsets. A low-dose noncontrast CT scan was applied for the attenuation correction of PET data. All subjects were carefully monitored during the scan and uptake phase, and encouraged to keep relaxed with minimal movement. When needed, sedation was initiated as late as possible prior to imaging (Varrone et al., 2009).

2.3 | Image analysis

All PET images were spatially normalized to the default adult template of tissue probability map (TPM) embedded in SPM12 package (Welcome Trust Centre for Neuroimaging, London, UK; http://www.fil.ion.ucl.ac.uk/spm). Then, 125 brain regions (excluding white matter, ventricle, and cerebrospinal fluid) were automatically segmented by using the neuromorphometrics atlas with maximum probability tissue labels (Figure 1). This labeled atlas originating from the OASIS project (http://www.oasis-brains.org/), was provided by Neuromorphometrics, Inc. (http://Neuromorphometrics.com/) under academic subscription. The ratio of each regional brain SUV_{mean} to the whole brain SUV_{mean} was calculated as the SUVR. Linear and nonlinear mathematic models were developed for each brain region to explore the variation in regional relative brain metabolism (SUVR) with age. The adopted nonlinear models were quadratic, cubic, logarithmic, inverse, power compound, logistic, growth, and exponential. Besides, all raw PET images were also spatially normalized to the corresponding

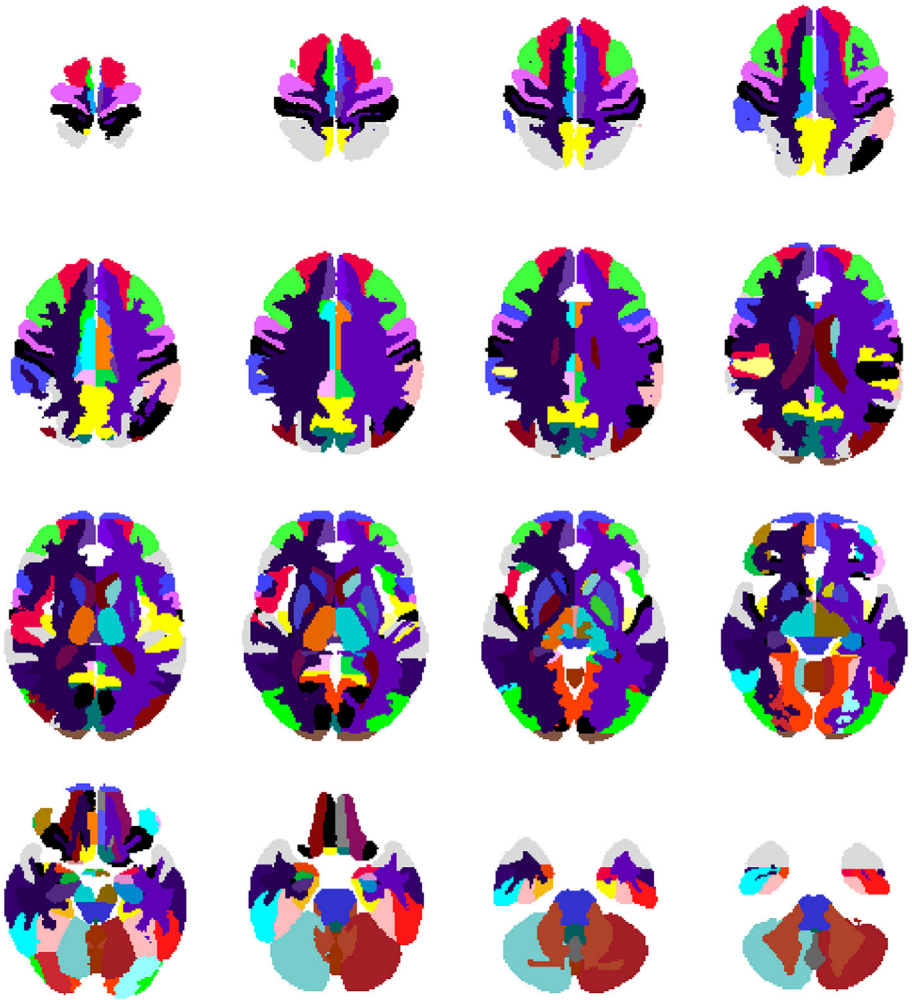

FIGURE 1 Neuromorphometrics atlas with maximum probability tissue labels embedded in SPM12 package.

home-made age-specific TPM templates for six age ranges, including 1, 2–3, 4–6, 7–10, 11–14, and 15–18 years of age (Figure 2) (Pilli et al., 2018; Zhu et al., 2017). To be specific, 1 year denoted the age range from 12 to 23 months, 2 to 3 years from 24 to 47 months, and so on.

All normalized PET data were then smoothed with an 8 mm isotropic Gaussian kernel to increase signal-to-noise ratio for statistical analysis. Subsequently, four types of SPM analysis procedures were performed by comparing each single pediatric epilepsy patient with control group (Kumar et al., 2010). SPMma was implemented by using age-matched controls (with the same age) with adult template, SPMaa using adult controls with adult template, SPMms using age-matched controls (with the same age) with age-specific template, and SPMas using adult controls with age-specific template. ANCOVA designed in SPM was utilized to identify difference in cerebral glucose metabolism between the male and female from pediatric control group, with the age as covariate (Kim et al., 2009). The difference in cerebral glucose metabolism between patients with lymphoma and other patients from pediatric control group was explored as well. Decreased or increased glucose metabolism was regarded as statistically significant, if the uncorrected p value was under .001 with cluster level above 50 voxels.

Brain ^{18}F-FDG PET images of both epilepsy and control groups were visually interpreted by two experienced nuclear medicine physicians separately. Discordant results were adjudicated by a third physician. The abnormal clusters in SPM analysis having a location concordant with visual assessment (or reassessment guided with the results of SPM analysis) were defined as true metabolic abnormalities, and the remaining as artifacts (Archambaud et al., 2013; Zhu et al., 2017). The significant hypometabolic or hypermetabolic clusters of SPM analysis and visual assessment were reported at 12 major brain regions (frontal lobe, temporal lobe, parietal lobe, occipital lobe, cingulate gyrus, and insular lobe or other regions in each hemisphere). In subjects with more than one region showing metabolic abnormalities, the severest one was selected for the further comparison between visual assessment and SPM analysis.

2.4 | Statistical analysis

All data were analyzed by the SPSS software (IBM SPSS Statistics, Version 25.0). Values of age were reported as median (interquartile range), while categorical variables as frequency. Comparison of gender or age between two groups was performed using chi-square test or

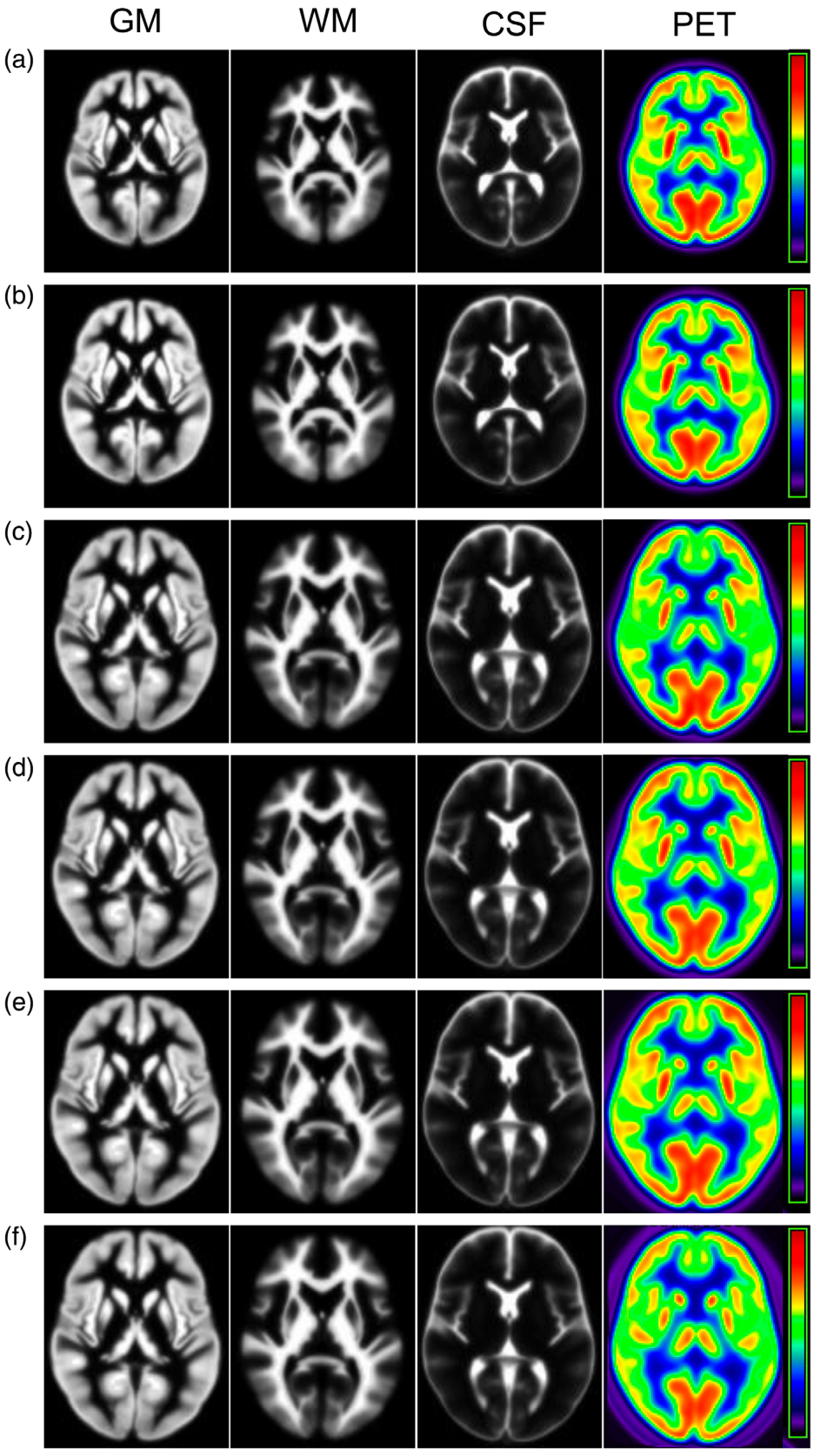

FIGURE 2 Age-specific brain templates for different age ranges. The tissue probability maps of gray matter (GM), white matter (WM), cerebrospinal fluid (CSF) and brain ^{18}F-fluorodeoxyglucose positron emission tomography ([^{18}F]-FDG PET) templates, were displayed for six age ranges: 1 (a), 2–3 (b), 4–6 (c), 7–10 (d), 11–14 (e), and 15–18 (f).

Mann–Whitney test, respectively. The numbers of brain regions affected by artifacts were compared among four types of SPM analysis procedures using Kruskal–Wallis test, followed by post hoc test when appropriate. The concordance between visual assessment and SPMms analysis was analyzed using kappa test. p value less than .05 was considered statistically significant.

3 | RESULTS

The demographics and age distribution of pediatric control and epilepsy groups are shown in Figure 3 and Table 1. No significant difference in gender ($\chi^2 = 0.097$, $p = .756$) or age ($p = .430$ for month and $p = .342$ for year, respectively) was found between these two groups.

For the pediatric control group, the optimal model for the effect of age (measured in month) on local cerebral glucose metabolism was cubic ($p < .05$) in 102 regions (Supplemental Table 1). The representative curves of regionally heterogeneous growth patterns are shown in Figure 4. Whereas, the effect of age on local cerebral glucose metabolism was not statistically significant in the remaining 23 regions, including left pallidum, bilateral anterior cingulate gyrus, right calcarine cortex, bilateral cuneus, right frontal operculum, bilateral frontal pole, right fusiform gyrus, left gyrus rectus, right inferior occipital gyrus, right inferior temporal gyrus, bilateral lateral orbital gyrus, right middle cingulate gyrus, bilateral medial orbital gyrus, bilateral occipital fusiform gyrus, bilateral posterior cingulate gyrus, and left planum polare. ANCOVA analysis did not show significant difference in cerebral glucose metabolism either between the male and female, or between patients with lymphoma and other patients.

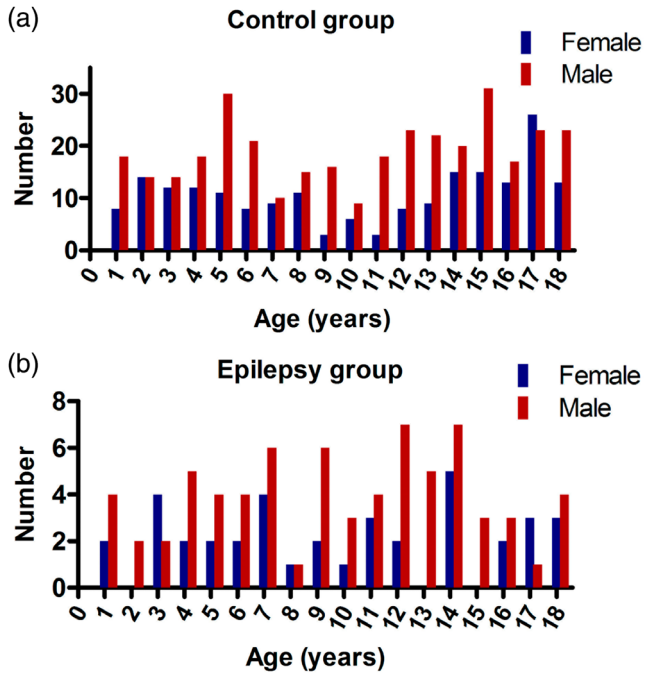

FIGURE 3 The age and gender distributions of pediatric control and epilepsy groups

For the voxel-wise analysis of brain ^{18}F-FDG PET images of epilepsy patients, significant difference in artifacts were observed among four types of SPM analysis procedures in each age range ($p < .05$ in each comparison, Table 2). Subsequent post hoc test was performed to compare any two procedures of SPM analysis. Any template being adopted, the artifacts were significantly less in procedures using age-matched controls than those using adult controls (i.e., SPMma vs. SPMaa, SPMma vs. SPMas, SPMms vs. SPMaa, and SPMms vs. SPMas) in all age ranges ($p < .001$ in each comparison), except in the age range of 15–18 ($p > .05$ in each comparison). Whereas, no significant difference was found in artifacts ($p = 1.000$ in each comparison), when compared procedures using different templates with the identical controls (i.e., SPMma vs. SPMms and SPMaa vs. SPMas) in all age ranges. Representative images of diverse age ranges are shown in Figure 5.

For the voxel-wise analysis of brain ^{18}F-FDG PET images of the controls, significant differences ($p < .001$, cluster >50 voxels) were found in cerebral metabolic patterns between pediatric controls aged 1–3 years and those aged 4–6 years (1928 voxels, Figure 6a), between those aged 4–6 years and those aged 7–10 years (2898 voxels, Figure 6b), between those aged 7–10 years and those aged 11–

TABLE 1 The demographics and clinical characteristics of pediatric control and epilepsy groups

Clinical characteristics	Control group ($n = 538$)	Epilepsy group ($n = 109$)	p value
Gender			
Female/male	196/342	38/71	.756
Age (months)	138 (65–186)	126 (75–173)	.430
Age (years)	11 (5–15)	10 (6–14)	.342
Disease category			
Non-Hodgkin's lymphoma	249		
Hodgkin's lymphoma	56		
Neuroblastoma[a]	59		
Fever of unknown origin	47		
LCH	19		
Nephroblastoma	17		
Germ cell tumor	14		
Hepatoblastoma	10		
The others	53		

Abbreviation: LCH, langerhans cell histiocytosis.
[a]Including ganglioneuro-blastoma.

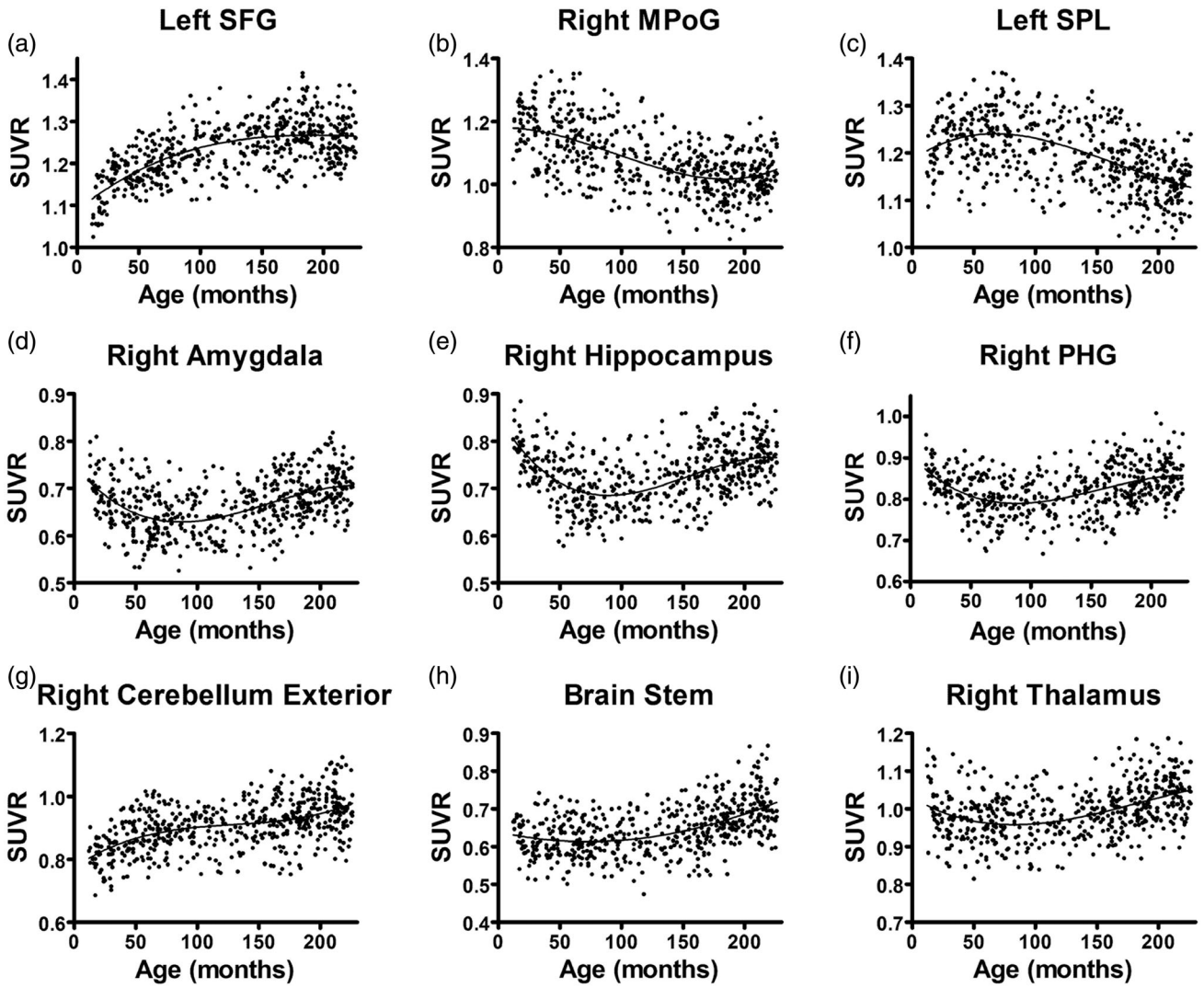

FIGURE 4 The cubic model for the effect of age on regional cerebral metabolism. The representative curves of regionally heterogeneous growth patterns were shown in the region of (a) left superior frontal gyrus (SFG) ($R^2 = .423$, $p < .001$); (b) right postcentral gyrus medial segment (MPoG) ($R^2 = .344$, $p < .001$); (c) left superior parietal lobule (SPL) ($R^2 = .309$, $p < .001$); (d) right amygdala ($R^2 = .240$, $p < .001$); (e) right hippocampus ($R^2 = .272$, $p < .001$); (f) right parahippocampal gyrus (PHG) ($R^2 = .170$, $p < .001$); (g) right cerebellum exterior ($R^2 = .272$, $p < .001$); (h) brain stem ($R^2 = .262$, $p < .001$); and (i) right thalamus ($R^2 = .184$, $p < .001$).

TABLE 2 Comparison of artifacts among four types of SPM analysis

	Age ranges (years)				
Comparisons	**1–18**	**1–6**	**7–10**	**11–14**	**15–18**
Kruskal–Wallis test	<0.001	<0.001	<0.001	<0.001	0.026
Post hoc test					
SPMma vs. SPMms	1.000	1.000	1.000	1.000	1.000
SPMma vs. SPMaa	<0.001	<0.001	<0.001	<0.001	0.519
SPMma vs. SPMas	<0.001	<0.001	<0.001	<0.001	0.427
SPMaa vs. SPMas	1.000	1.000	1.000	1.000	1.000
SPMms vs. SPMaa	<0.001	<0.001	<0.001	<0.001	0.100
SPMms vs. SPMas	<0.001	<0.001	<0.001	<0.001	0.078

Note: SPMma was implemented by using age-matched controls with adult template, SPMaa using adult controls with adult template, SPMms using age-matched controls with age-specific template, and SPMas using adult controls with age-specific template.

Abbreviation: SPM, statistical parametric mapping.

14 years (35,473 voxels, Figure 6c), and between those aged 11–14 years and those aged 15–18 years (11,250 voxels, Figure 6d). Moreover, differences in cerebral metabolic patterns between the pediatric controls in each age group and the adult controls gradually decreased with age ($r = -.942$, $p < .001$, Figure 7).

Cerebral metabolic abnormalities were identified by SPMms analysis in 99 patients (90.8%), including 93 with hypometabolism and 6 with hypermetabolism (Tables 3 and 4). Visual assessment indicated abnormal metabolism in 96 patients (88.1%), including 90 with hypometabolism and 6 with hypermetabolism. A concordant lateralization for abnormal cerebral metabolism between the SPMms analysis and visual assessment was obtained in 104 patients ($\kappa = 0.922$, $p < .001$, Table 3), while a concordant localization in 104 patients as well ($\kappa = 0.936$, $p < .001$, Table 4). Among the 93 patients with hypometabolism identified by SPMms analysis, primary visual assessment failed to manifest any abnormal metabolism in 4 patients (Table 4 and Figure 8). These subtle lesions were located at orbitofrontal gyrus and gyrus rectus in two patients, and cingulate gyrus in two patients, and representative images are shown in Supplemental Figure 1. In contrast, among the 90 patients with hypometabolism identified by visual assessment, the hypometabolism of 1 patient was not detected by SPMms analysis.

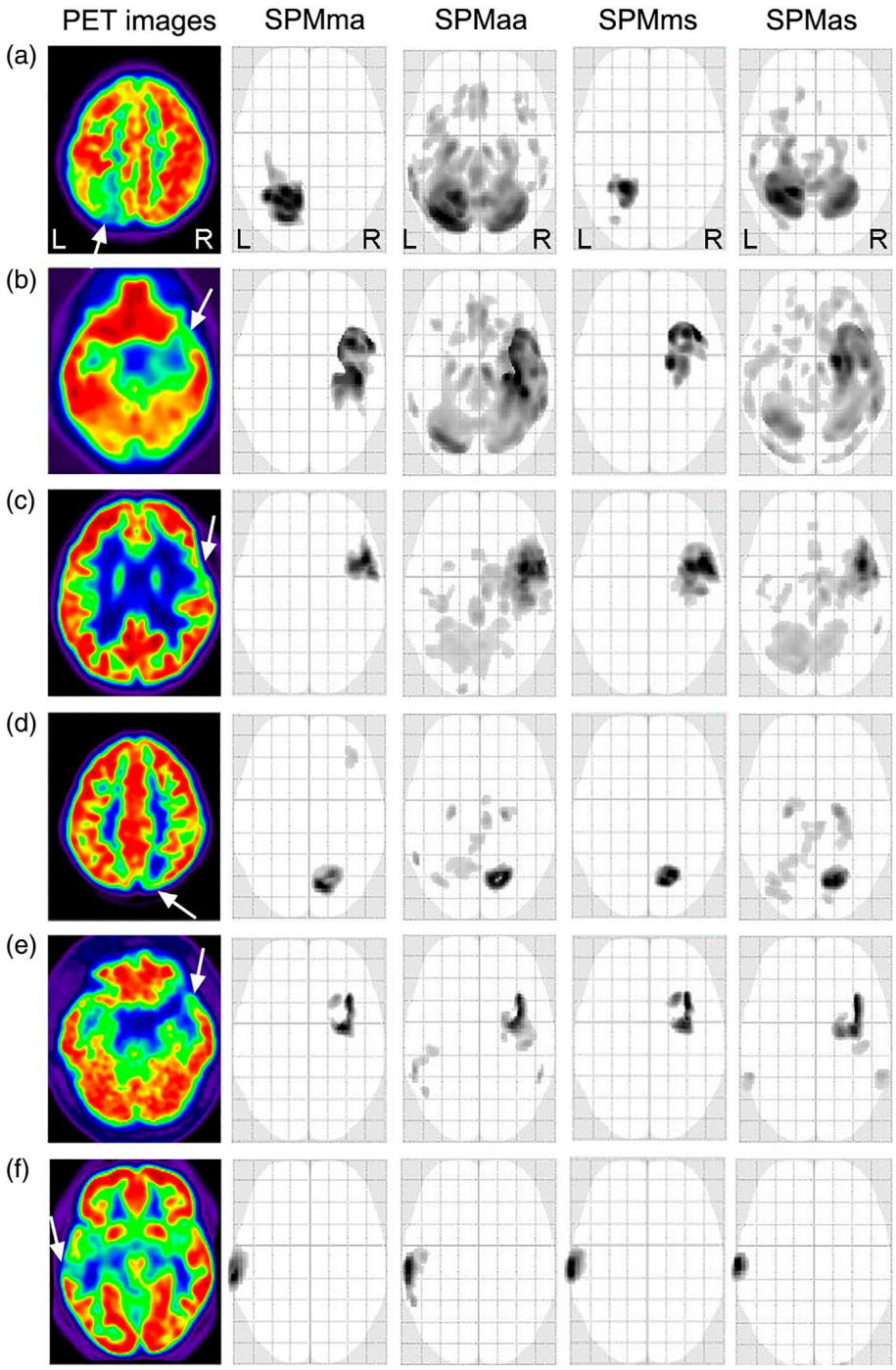

FIGURE 5 Comparison of artifacts among four types of statistical parametric mapping (SPM) analysis procedures. The representative positron emission tomography (PET) images (solid arrow indicating the focal hypometabolism) and glass brain displays of corresponding SPM analysis were demonstrated for six age ranges: 1 (a), 2–3 (b), 4–6 (c), 7–10 (d), 11–14 (e), and 15–18 (f). SPMma was implemented by using age-matched controls with adult template, SPMaa using adult controls with adult template, SPMms using age-matched controls with age-specific template, and SPMas using adult controls with age-specific template. The abnormal clusters in SPM analysis having a cerebral location concordant with visual assessment were defined as true metabolic abnormalities, while the remaining artifacts.

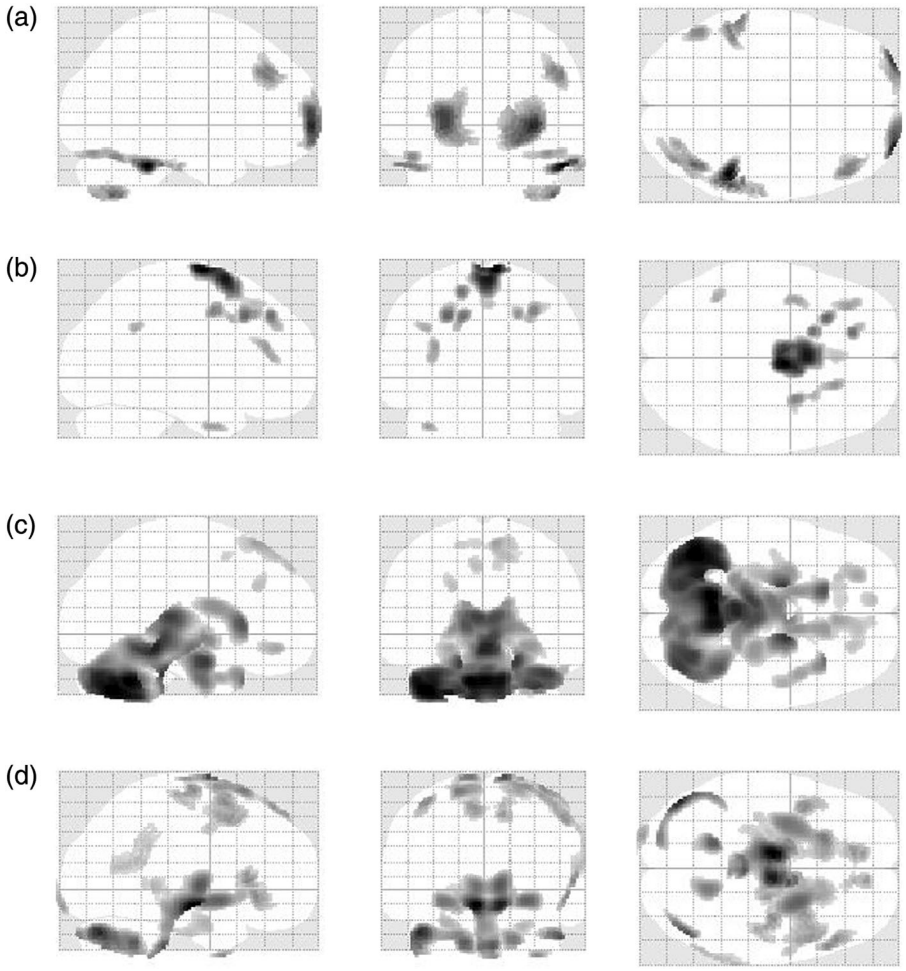

FIGURE 6 Comparison of cerebral metabolic patterns among patients with different age ranges. Significant differences ($p < .001$, cluster >50 voxels) were found in cerebral metabolic patterns between pediatric controls aged 1–3 years and those aged 4–6 years (a, 1928 voxels), between those aged 4–6 years and those aged 7–10 years (b, 2898 voxels), between those aged 7–10 years and those aged 11–14 years (c, 35,473 voxels), and between those aged 11–14 years and those aged 15–18 years (d, 11,250 voxels).

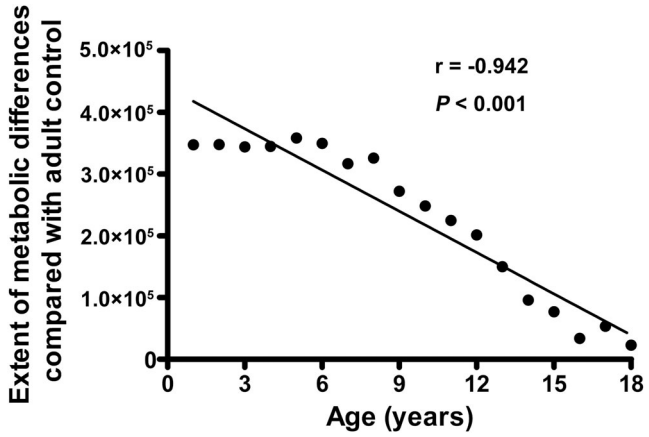

FIGURE 7 Differences in cerebral metabolic patterns between the pediatric controls in each age group and the adult control. The extent (in voxels) of metabolic differences compared with adult control was significantly negatively correlated with age ($r = -.942$, $p < .001$).

4 | DISCUSSION

In this retrospective study, we established pediatric control database of brain ^{18}F-FDG PET images, accompanied by corresponding age-specific templates for six age ranges. Although age-matched control is essential for the SPM analysis of brain ^{18}F-FDG PET images in pediatric epilepsy patients ≤14-year-old, age-specific template is not mandatory. Besides, the thinner the age stratification for age-matched control group, the more reliable and precise the results in the SPM analysis.

In several studies, adult control group and adult brain template were utilized in the SPM analysis for interpreting ^{18}F-FDG PET images of pediatric patients with epilepsy (Kumar et al., 2010; Lee et al., 2005; Muzik et al., 2000). However, in this instance, the age-related alterations of brain contour and regionally heterogeneous growth patterns of cerebral glucose metabolism may induce dramatic artifacts in the image processing procedure (London & Howman-Giles, 2015; Shan et al., 2014; Trotta et al., 2016; Turpin et al., 2018). Due to the ethical consideration, brain ^{18}F-FDG PET data sets derived from completely healthy age-matched pediatric controls are not available. A variety of control groups with "pseudo-normal" pediatric subjects have been screened from epilepsy patients with normal-appearing cerebral metabolism, deaf children or extracranial malignancy patients without brain involvement (Archambaud et al., 2013; Kang et al., 2004; Zhu et al., 2017).

A potential advantage of using "pseudo-normal" epilepsy patients as control is that the effect of the antiepileptics on cerebral metabolism could be partially eliminated in the comparison between groups (Archambaud et al., 2013). Whereas the present study indicated that

TABLE 3 Comparison of lateralization value between visual assessment and SPMms analysis

Visual assessment	SPMms analysis			Total
	Negative	Left hemisphere	Right hemisphere	
Negative	9	1	3	13
Left hemisphere	0	46	0	46
Right hemisphere	1	0	49	50
Total	10	47	52	109

Note: $\kappa = 0.922$, $p < .001$.
Abbreviation: SPM, statistical parametric mapping.

TABLE 4 Comparison of localization value between visual assessment and SPMms analysis

Visual assessment	SPMms analysis						Total
	Negative	F	P	T	O	CI	
Negative	9	2	0	0	0	2	13
F	0	34[a]	0	0	0	0	34
P	0	0	13	0	0	0	13
T	1	0	0	42[b]	0	0	43
O	0	0	0	0	2	0	2
CI	0	0	0	0	0	4	4
Total	10	36	13	42	2	6	109

Note: $\kappa = 0.936$, $p < .001$; F = frontal lobe; P = parietal lobe; T = temporal lobe; O = occipital lobe; CI = cingulate gyrus and insular lobe.
Abbreviation: SPM, statistical parametric mapping.
[a]One patient with hypermetabolism.
[b]Five patients with hypermetabolism.

SPM analysis may provide the possibility to detect several subtle metabolic abnormalities missed by routine visual assessment, which was also manifested in previous studies (Bernasconi et al., 2016; Zhu et al., 2017). Besides, as cortical plasticity of cerebral auditory system can be induced by auditory stimulation, the brain development of deaf children differs from that of healthy children undoubtedly (Yoshida et al., 2017). Therefore, it is preferable to introduce pediatric patients without brain involvement as age-matched control for the voxel-wise analysis of brain ^{18}F-FDG PET images.

Few studies on the normative database of ^{18}F-FDG PET images in pediatric subjects have been performed (De Blasi et al., 2018; Hua et al., 2015; London & Howman-Giles, 2014, 2015; Shan et al., 2014). To our best knowledge, our control data sets provide the largest sample size, which were further classified into each age for pediatric subjects. To verify the feasibility of the selected age-matched "pseudo-control" group in our study, the localization value for abnormal metabolism of pediatric epilepsy patients was compared between routine visual assessment and age-matched SPM analysis. Apart from an equivalent diagnostic efficacy compared with visual assessment, SPM analysis allowed the detection of focal subtle hypometabolism, which might be missed in the primary visual assessment (Bernasconi et al., 2016; Kumar et al., 2010; Zhu et al., 2017).

The prominent finding in the current study was the necessity of using age-matched control for the SPM analysis in pediatric patients ≤14-year-old. In a previous study, a "pseudo-control" data set including 112 subjects (6–20 years old) were roughly divided into two groups based on 10-year-old cutoff (De Blasi et al., 2018). However, it could hardly discern the difference in practically applicable value of age-matched control data sets between 11–14 and 15–18 years old. This design flaw also existed in other studies (Archambaud et al., 2013; Mazzuca et al., 2011). By virtue of sufficiently large sample size, the age stratification in our study must be more precise than those using only single or double age ranges.

Theoretically, age-specific brain templates could minimize the errors in the process for normalizing brain ^{18}F-FDG PET images of pediatric subjects. It was suggested that normalization procedures could induce prominent errors in pediatric subjects below 6-year-old, if using an adult template (Muzik et al., 2000). However, this default template embedded in the old SPM96 version was produced based on ^{15}O-H_2O PET data. Only a few studies have developed age-specific brain templates for voxel-wise statistical analysis so far (Archambaud et al., 2013; De Blasi et al., 2018; Jeong et al., 2017; Mazzuca et al., 2011; Pilli et al., 2018; Zhu et al., 2017). Artifacts in SPM analysis for pediatric subjects might be also partly derived from the comparison procedure with an adult control group. As pediatric brain templates were commonly applied in combination with the age-matched control group in SPM analysis, whether template or control should be mainly responsible for the aberrant artifacts remains elusive. In our current study, remarkably, no significant contribution of age-specific templates was found for the artifacts derived from SPM

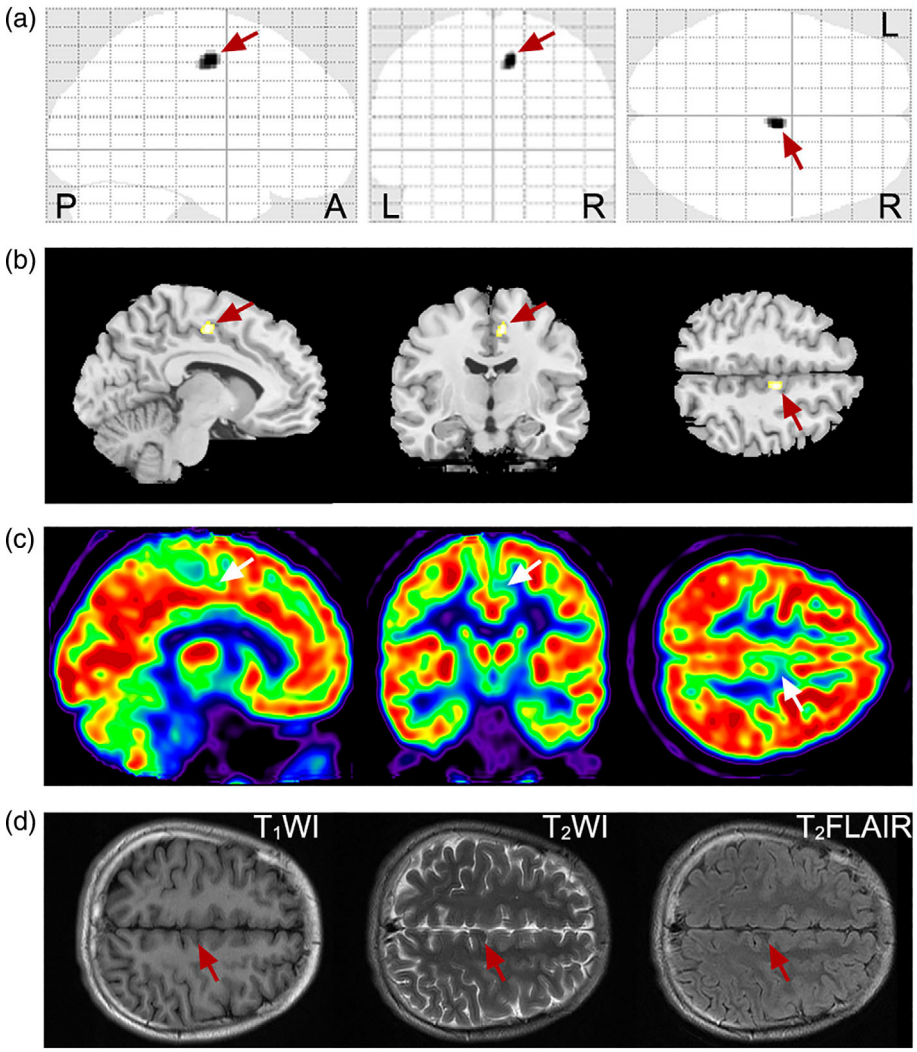

FIGURE 8 Added value of statistical parametric mapping (SPM) analysis in the interpretation for brain ^{18}F-fluorodeoxyglucose positron emission tomography ([^{18}F]-FDG PET) images. A 15-year-old boy affected by drug-resistant epilepsy received comprehensive presurgical evaluation. The statistical results of SPM analysis for brain [^{18}F]FDG PET data displayed on glass brain (a) or coregistered with MR template (b), showed a focal hypometabolism in cingulate gyrus (solid arrow), which was missed in the primary visual assessment (c). T1 isointensity, T2 hypointensity, and T2-FLAIR hypointensity were also detected in cingulate gyrus (d)

analysis. We speculated that the errors resulted from the normalization procedure could be offset to some extent, when the two compared groups were normalized to the identical template.

Another issue is about the intensity normalization for PET images. It should be noted that most of the subjects were proven or suspected extracranial malignancy in the current study. Significantly negative correlation between total lesion glycolysis and brain glucose uptake has been reported in oncology patients without brain involvement (Hanaoka et al., 2010). Considering the competition for capturing FDG between the tumor and the brain, the value of SUV commonly used in clinical practice, should be unsuitable for the data comparison among these patients with varying degrees of tumor burdens (Foster et al., 2014). This dilemma might be solved by using the absolute quantitative parameter of cerebral metabolic rate of glucose. However, this "gold standard" approach cannot be acquired from routine clinical PET study. Therefore, in the process of voxel-wise analysis, the intensity in each voxel was normalized by the whole brain before the implementation of comparison, in order to eliminate the effect of discrepancy in whole-brain "input" of FDG (Signorini et al., 1999). In view of this advantage, VOI-based analysis was also performed with a similar process by choosing the whole brain SUV_{mean} as the reference to calculate the SUVR.

There were some limitations existed in our study. First, "pseudo-normal" pediatric controls with extracranial disease were merely surrogates for healthy subjects. However, factors affecting cerebral glucose metabolism were precluded in the selection of age-matched control data sets, which were considered to closely represent normal cerebral FDG distribution in their age. Practical application of this "pseudo-control" in SPM analysis has been also verified (De Blasi et al., 2018; Zhu et al., 2017). Second, all the separated brain PET images were acquired immediately after the whole-body PET/CT scan, which started 60 min after FDG injection in the control group. Thus, the difference in the time interval between the control group and the epileptic group with dedicated brain scan was about 10 min. The uptake pattern of FDG in brain may vary with time after injection, for example, between the time points of 30 and 60 min (Ishii et al., 2002). Although the metabolic differences within 10 min cannot be ruled out yet, the optimal choice for pediatric control group without any cerebral pathology should be derived from patients receiving whole-body ^{18}F-FDG PET/CT study as far as we know. Third, factorial

design cannot be performed to explore the effects of control group, template, and their interaction effects on the SPM analysis for pediatric subjects, due to the skew distribution and unequal variances of data. However, alternative nonparametric test, post hoc test after Kruskal–Wallis test, clearly discriminated the divergent impacts of control group and template on the voxel-wise analysis for pediatric subjects.

5 | CONCLUSIONS

Age-matched control rather than age-specific template is essential for the SPM analysis of brain ^{18}F-FDG images in pediatric epilepsy patients ≤14-year-old. Besides, the age stratification for pediatric control database should be divided as many layers as possible, due to the regionally heterogeneous growth patterns of cerebral glucose metabolism.

CONFLICT OF INTEREST

The authors declare no potential conflict of interest.

DATA AVAILABILITY STATEMENT

The data sets generated during and/or analyzed during the current study are not publicly available, but are available from the corresponding author on reasonable request.

PATIENT CONSENT STATEMENT

The claim for informed consent was waived.

ORCID

Yuankai Zhu https://orcid.org/0000-0003-2219-251X
Xiaohua Zhu https://orcid.org/0000-0003-0495-9510

REFERENCES

Archambaud, F., Bouilleret, V., Hertz-Pannier, L., Chaumet-Riffaud, P., Rodrigo, S., Dulac, O., Chassoux, F., & Chiron, C. (2013). Optimizing statistical parametric mapping analysis of 18F-FDG PET in children. *EJNMMI Res*, *3*(1), 2. https://doi.org/10.1186/2191-219X-3-2

Beghi, E., Giussani, G., Nichols, E., Abd-Allah, F., Abdela, J., Abdelalim, A., Abraha, H. N., Adib, M. G., Agrawal, S., Alahdab, F., Awasthi, A., Ayele, Y., Barboza, M. A., Belachew, A. B., Biadgo, B., Bijani, A., Bitew, H., Carvalho, F., Chaiah, Y., … Murray, C. J. L. (2019). Global, regional, and national burden of epilepsy, 1990–2016: a systematic analysis for the Global Burden of Disease Study 2016. *The Lancet Neurology*, *18*(4), 357–375. https://doi.org/10.1016/s1474-4422(18)30454-x

Bernasconi, N., Mayoral, M., Marti-Fuster, B., Carreño, M., Carrasco, J. L., Bargalló, N., Donaire, A., Rumià, J., Perissinotti, A., Lomeña, F., Pintor, L., Boget, T., & Setoain, X. (2016). Seizure-onset zone localization by statistical parametric mapping in visually normal (18) F-FDG PET studies. *Epilepsia*, *57*(8), 1236–1244. https://doi.org/10.1111/epi.13427

Chassoux, F., Rodrigo, S., Semah, F., Beuvon, F., Landre, E., Devaux, B., Turak, B., Mellerio, C., Meder, J. F., Roux, F. X., Daumas-Duport, C., Merlet, P., Dulac, O., & Chiron, C. (2010). FDG-PET improves surgical outcome in negative MRI Taylor-type focal cortical dysplasias. *Neurology*, *75*(24), 2168–2175. https://doi.org/10.1212/WNL.0b013e31820203a9

De Blasi, B., Barnes, A., Galazzo, I. B., Hua, C. H., Shulkin, B., Koepp, M., & Tisdall, M. (2018). Age-specific (18)F-FDG image processing pipelines and analysis are essential for individual mapping of seizure foci in pediatric patients with intractable epilepsy. *Journal of Nuclear Medicine*, *59*(10), 1590–1596. https://doi.org/10.2967/jnumed.117.203950

Foster, B., Bagci, U., Mansoor, A., Xu, Z., & Mollura, D. J. (2014). A review on segmentation of positron emission tomography images. *Computers in Biology and Medicine*, *50*, 76–96. https://doi.org/10.1016/j.compbiomed.2014.04.014

Gelfand, M. J., Parisi, M. T., & Treves, S. T. (2011). Pediatric radiopharmaceutical administered doses: 2010 North American consensus guidelines. *Journal of Nuclear Medicine*, *52*(2), 318–322. https://doi.org/10.2967/jnumed.110.084327

Hanaoka, K., Hosono, M., Shimono, T., Usami, K., Komeya, Y., Tsuchiya, N., Yamazoe, Y., Ishii, K., Tatsumi, Y., & Sumita, M. (2010). Decreased brain FDG uptake in patients with extensive non-Hodgkin's lymphoma lesions. *Annals of Nuclear Medicine*, *24*(10), 707–711. https://doi.org/10.1007/s12149-010-0415-5

Hua, C., Merchant, T. E., Li, X., Li, Y., & Shulkin, B. L. (2015). Establishing age-associated normative ranges of the cerebral 18F-FDG uptake ratio in children. *Journal of Nuclear Medicine*, *56*(4), 575–579. https://doi.org/10.2967/jnumed.114.146993

Ishii, K., Sakamoto, S., Hosaka, K., Mori, T., & Sasaki, M. (2002). Variation in FDG uptakes in different regions in normal human brain as a function of the time (30 and 60 minutes) after injection of FDG. *Annals of Nuclear Medicine*, *16*(4), 299–301. https://doi.org/10.1007/BF03000112

Jeong, J.-W., Asano, E., Kumar Pilli, V., Nakai, Y., Chugani, H. T., & Juhász, C. (2017). Objective 3D surface evaluation of intracranial electrophysiologic correlates of cerebral glucose metabolic abnormalities in children with focal epilepsy. *Human Brain Mapping*, *38*(6), 3098–3112. https://doi.org/10.1002/hbm.23577

Kang, E., Lee, D. S., Kang, H., Lee, J. S., Oh, S. H., Lee, M. C., & Kim, C. S. (2004). Age-associated changes of cerebral glucose metabolic activity in both male and female deaf children: Parametric analysis using objective volume of interest and voxel-based mapping. *NeuroImage*, *22*(4), 1543–1553. https://doi.org/10.1016/j.neuroimage.2004.04.010

Kim, I. J., Kim, S. J., & Kim, Y. K. (2009). Age- and sex-associated changes in cerebral glucose metabolism in normal healthy subjects: Statistical parametric mapping analysis of F-18 fluorodeoxyglucose brain positron emission tomography. *Acta Radiologica*, *50*(10), 1169–1174. https://doi.org/10.3109/02841850903258058

Kumar, A., Alhourani, H., Abdelkader, A., Shah, A. K., Juhász, C., & Basha, M. M. (2021). Frontal lobe hypometabolism associated with Sudden Unexpected Death in Epilepsy (SUDEP) risk: An objective PET study. *Epilepsy & Behavior*, *122*, 108185. https://doi.org/10.1016/j.yebeh.2021.108185

Kumar, A., Juhasz, C., Asano, E., Sood, S., Muzik, O., & Chugani, H. T. (2010). Objective detection of epileptic foci by 18F-FDG PET in children undergoing epilepsy surgery. *Journal of Nuclear Medicine*, *51*(12), 1901–1907. https://doi.org/10.2967/jnumed.110.075390

Kwan, P., Arzimanoglou, A., Berg, A. T., Brodie, M. J., Allen Hauser, W., Mathern, G., Moshe, S. L., Perucca, E., Wiebe, S., & French, J. (2010). Definition of drug resistant epilepsy: consensus proposal by the ad hoc Task Force of the ILAE Commission on Therapeutic Strategies. *Epilepsia*, *51*(6), 1069–1077. https://doi.org/10.1111/j.1528-1167.2009.02397.x

Lagarde, S., Boucekine, M., McGonigal, A., Carron, R., Scavarda, D., Trebuchon, A., Milh, M., Boyer, L., Bartolomei, F., & Guedj, E. (2020). Relationship between PET metabolism and SEEG epileptogenicity in focal lesional epilepsy. *European Journal of Nuclear Medicine and Molecular Imaging*, *47*(13), 3130–3142. https://doi.org/10.1007/s00259-020-04791-1

Lamberink, H., Otte, W., Blümcke, I., & Braun, K. (2020). Seizure outcome and use of antiepileptic drugs after epilepsy surgery according to histopathological diagnosis: A retrospective multicentre cohort study. *Lancet Neurology*, *19*(9), 748–757. https://doi.org/10.1016/s1474-4422(20)30220-9

Lee, J. J., Kang, W. J., Lee, D. S., Lee, J. S., Hwang, H., Kim, K. J., Hwang, Y. S., Chung, J. K., & Lee, M. C. (2005). Diagnostic performance of 18F-FDG PET and ictal 99mTc-HMPAO SPET in pediatric temporal lobe epilepsy: quantitative analysis by statistical parametric mapping, statistical probabilistic anatomical map, and subtraction ictal SPET. *Seizure*, *14*(3), 213–220. https://doi.org/10.1016/j.seizure.2005.01.010

London, K., & Howman-Giles, R. (2014). Normal cerebral FDG uptake during childhood. *European Journal of Nuclear Medicine and Molecular Imaging*, *41*(4), 723–735. https://doi.org/10.1007/s00259-013-2639-9

London, K., & Howman-Giles, R. (2015). Voxel-based analysis of normal cerebral [18F]FDG uptake during childhood using statistical parametric mapping. *NeuroImage*, *106*, 264–271. https://doi.org/10.1016/j.neuroimage.2014.11.047

Mazzuca, M., Jambaque, I., Hertz-Pannier, L., Bouilleret, V., Archambaud, F., Caviness, V., Rodrigo, S., Dulac, O., & Chiron, C. (2011). 18F-FDG PET reveals frontotemporal dysfunction in children with fever-induced refractory epileptic encephalopathy. *Journal of Nuclear Medicine*, *52*(1), 40–47. https://doi.org/10.2967/jnumed.110.077214

Muzik, O., Chugani, D. C., Juhasz, C., Shen, C., & Chugani, H. T. (2000). Statistical parametric mapping: Assessment of application in children. *NeuroImage*, *12*(5), 538–549. https://doi.org/10.1006/nimg.2000.0651

Pilli, V. K., Jeong, J. W., Konka, P., Kumar, A., Chugani, H. T., & Juhász, C. (2018). Objective PET study of glucose metabolism asymmetries in children with epilepsy: Implications for normal brain development. *Human Brain Mapping*, *40*(1), 53–64. https://doi.org/10.1002/hbm.24354

Shan, Z. Y., Leiker, A. J., Onar-Thomas, A., Li, Y., Feng, T., Reddick, W. E., Reutens, D. C., & Shulkin, B. L. (2014). Cerebral glucose metabolism on positron emission tomography of children. *Human Brain Mapping*, *35*(5), 2297–2309. https://doi.org/10.1002/hbm.22328

Signorini, M., Paulesu, E., Friston, K., Perani, D., Colleluori, A., Lucignani, G., Grassi, F., Bettinardi, V., Frackowiak, R. S., & Fazio, F. (1999). Rapid assessment of regional cerebral metabolic abnormalities in single subjects with quantitative and nonquantitative [18F]FDG PET: A clinical validation of statistical parametric mapping. *Neuroimage*, *9*(1), 63–80. https://doi.org/10.1006/nimg.1998.0381.

Trotta, N., Archambaud, F., Goldman, S., Baete, K., Van Laere, K., Wens, V., Van Bogaert, P., Chiron, C., & De Tiège, X. (2016). Functional integration changes in regional brain glucose metabolism from childhood to adulthood. *Human Brain Mapping*, *37*(8), 3017–3030. https://doi.org/10.1002/hbm.23223

Turpin, S., Martineau, P., Levasseur, M.-A., & Lambert, R. (2018). Modeling the effects of age and sex on normal pediatric brain metabolism using 18F-FDG PET/CT. *Journal of Nuclear Medicine*, *59*(7), 1118–1124. https://doi.org/10.2967/jnumed.117.201889

Varrone, A., Asenbaum, S., Vander Borght, T., Booij, J., Nobili, F., Nagren, K., Darcourt, J., Kapucu, O. L., Tatsch, K., Bartenstein, P., & Van Laere, K. (2009). EANM procedure guidelines for PET brain imaging using [18F]FDG, version 2. *European Journal of Nuclear Medicine and Molecular Imaging*, *36*(12), 2103–2110. https://doi.org/10.1007/s00259-009-1264-0

Verrotti, A., & Mazzocchetti, C. (2016). Epilepsy: Beyond seizures—The importance of comorbidities in epilepsy. *Nature Reviews. Neurology*, *12*(10), 559–560. https://doi.org/10.1038/nrneurol.2016.135

Yoshida, H., Takahashi, H., Kanda, Y., & Chiba, K. (2017). PET-CT observations of cortical activity in pre-lingually deaf adolescent and adult patients with cochlear implantation. *Acta Oto-Laryngologica*, *137*(5), 464–470. https://doi.org/10.1080/00016489.2016.1253868

Zhu, Y., Feng, J., Wu, S., Hou, H., Ji, J., Zhang, K., Chen, Q., Chen, L., Cheng, H., Gao, L., Chen, Z., Zhang, H., & Tian, M. (2017). Glucose metabolic profile by visual assessment combined with statistical parametric mapping analysis in pediatric patients with epilepsy. *Journal of Nuclear Medicine*, *58*(8), 1293–1299. https://doi.org/10.2967/jnumed.116.187492

SUPPORTING INFORMATION

Additional supporting information can be found online in the Supporting Information section at the end of this article.

How to cite this article: Zhu, Y., Ruan, G., Zou, S., Liu, L., & Zhu, X. (2023). Age-matched control or age-specific template, which is essential for voxel-wise analysis of cerebral metabolism abnormality in pediatric patients with epilepsy? *Human Brain Mapping*, *44*(2), 472–483. https://doi.org/10.1002/hbm.26063